Haplo-insufficiency of Profilin1 in vascular endothelial cells is beneficial but not sufficient to confer protection against experimentally induced atherosclerosis

Abigail Allen-Gondringer[1], Partha Dutta[1,2,] Partha Roy[1,3]

[1] Bioengineering, [2]Medicine [3] Pathology, University of Pittsburgh, Pittsburgh, PA

Correspondence: Partha Roy, 306 CNBIO, 300 Technology Drive, Pittsburgh, PA 15219

Email: par19@pitt.edu

Running Title: Vascular endothelial Profilin1 and atherosclerosis

Abstract

Actin cytoskeleton plays an important role in various aspects of atherosclerosis, a key driver of ischemic heart disease. Actin-binding protein Profilin1 (Pfn1) is overexpressed in atherosclerotic plaques in human disease, and Pfn1, when partially depleted globally in all cell types, confers atheroprotection *in vivo*. This study investigates the impact of endothelial cell (EC)-specific partial loss of Pfn1 expression in atherosclerosis development. We utilized mice engineered for conditional heterozygous knockout of the Pfn1 gene in ECs with atherosclerosis induced by PCSK9-encoding adeno-associated virus-mediated depletion of hepatic LDL receptor combined with high-cholesterol diet. Our studies show that partial depletion of EC Pfn1 has certain beneficial effects marked by dampening of select pro-atherogenic cytokines (CXCL10 and IL7) with concomitant reduction in cytotoxic T cell abundance but is not sufficient to reduce hyperlipidemia and confer atheroprotection *in vivo*. In light of these findings, we conclude that atheroprotective phenotype conferred by global Pfn1 haplo-insufficiency requires contributions of additional cell types that are relevant for atherosclerosis progression.

Keywords: Profilin1, atherosclerosis, cytotoxic T cells, CXCL10, IL7

Introduction

Cardiovascular diseases are a leading cause of death world-wide, contributing to approximately 17.9 million deaths a year [1]. The most common form, ischemic heart disease, remains the leading cause of cardiovascular-related death, and develops due to atherosclerotic plaque formation [2]. Atherosclerosis begins with fatty streak deposition, appearing in clinically relevant locations including aortic, coronary, and cerebellar arteries as early as age 30-40 years in humans [3]. Over time, fatty streaks develop into fibrotic plaques composed of extracellular matrix and necrotic cellular deposits, smooth muscle cells (SMCs) and immune cells. Immune cell sub-populations are characterized by infiltration of lipid-rich macrophagic foam cells, cytotoxic T lymphocytes, granulocytes, and other antigen presenting cells (APCs) [3], [4]. An early contributor to fatty streaks and plaque development is EC dysfunction. In the healthy endothelium, atheroprotective nitric oxide (NO) released by constitutive endothelial nitric oxide synthase (eNOS)[5] regulates expression of endothelial cell adhesion molecules (CAMs, i.e. VCAM-1, ICAM-1), while eNOS dysfunction in the vasculature (signified by a decrease in bioavailable nitric oxide (NO))[6] may enhance levels of VCAM-1 and ICAM-1, inciting local immune invasion and inflammation[7].

Actin cytoskeleton plays an important role in various aspects of atherosclerosis. For example, remodeling of actin cytoskeleton is largely responsible for pro-atherogenic morphological changes and dysfunction (characterized by impaired barrier function) of ECs in response to turbulent flow[8], [9]. Actin regulatory proteins control EC stiffness, in turn impacting clustering of cell surface adhesion molecules and transendothelial migration of immune cells [10]. Other aspects of atherosclerosis, such as polarization and lipid processing by macrophages, are sensitive to the state of actin cytoskeleton in immune cells [11], [12]. Overexpression of actin-binding protein Profilin1

(Pfn1 - an important promoter of actin polymerization in cells) in atherosclerotic plaques as well as increased circulating level of Pfn1 in the serum are features of human atherosclerosis[13]. In atherosclerotic plaques, Pfn1 abundance is elevated in both intracellular and extracellular spaces, and *in vitro* studies provide evidence for Pfn1's ability to stimulate vascular smooth muscle cell migration and proliferation (features of atherosclerosis) utilizing an extracellular mode of action[14]. High-fat diet-induced atherosclerosis in low-density lipoprotein receptor (LDLR) knockout ($LDLR^{-/-}$) mice also leads to a trend of Pfn1 expression increase in atherosclerotic blood vessels mimicking the human disease. Furthermore, when Pfn1 expression is partially depleted globally in all cell types by heterozygous gene deletion in $LDLR^{-/-}$ mice, it results in reduced severity of atherosclerosis marked by smaller plaque size, lower VCAM-1 expression, and diminished vascular infiltration by macrophages [15]. However, since atherosclerosis involves altered activities of a number of different cell types including vascular EC, immune cells (monocytes/macrophages, neutrophils and various subpopulation of T cells) and vascular smooth muscle cells, Pfn1 downregulation in which specific cell type is primarily responsible for atheroprotective effect in $Pfn1^{+/-}$ mice remained unclear. Our recent studies show that triggering complete loss of vascular EC Pfn1 has a profound immunological consequence providing evidence for Pfn1 as an important mediator of vascular EC-immune cell crosstalk[16]. Given these findings, we sought to investigate whether haplo-insufficiency of Pfn1 in vascular ECs alone has any beneficial effect in experimentally induced atherosclerosis.

Material and Methods

In vivo experiments. $Pfn1^{flox/flox}$:CDH5-Cre-ERT2 mice, as previously described[16]–[18] were backcrossed into C57Bl/6 background for 5-6 generations to generate $Pfn1^{flox/WT}$:CDH5-Cre-

ERT2 mice (WT – wild-type allele). These mice (both male and female) when 4-6 weeks old, were subjected to intraperitoneal injection of 100µl tamoxifen (dissolved in peanut oil at a concentration of 10 mg/ml) daily over a course of five days to achieve Cre-mediated deletion of the floxed Pfn1 allele (denoted as $^{Pfn1+/-(EC)}$ hereon), as we had done before [16]. Control animals (any Pfn1 genotype without Cre expression - denoted as $Pfn1^{+/+}$ hereon) were also subjected to tamoxifen administration in a similar manner. Details of genotyping primers to confirm floxed alleles of Pfn1, Cre, and Cre- mediated excision of Pfn1 are described in [19]. To confirm Cre-mediated downregulation of Pfn1 expression at the protein level, CD31+ ECs were isolated from the kidneys (a vascular-rich organ) of select $Pfn1^{+/+}$ and $Pfn1^{+/-(EC)}$ mice, and cultured for 7 days before performing immunoblot analyses of total cell extracts as per our previously described protocol [16]. One month after gene excision, mice were subjected to intraperitoneal injection of $2x10^{11}$ PFU AAV8 encoding constitutively active mutant (D377Y) form of mouse PCSK9 (Proprotein convertase subtilisin/kexin type-9; referred to as AAV8-mPCSK9 from hereon; Vector Biolabs, Malvern PA) and fed a high-cholesterol diet (HCD - D12336i, Research Diets, New Brunswick NJ) for 3 months to develop atherosclerosis[20], [21]. For confirmation of LDLR knockout and serum cholesterol elevation, animals were similarly injected with GFP-encoding AAV8 as control [22]. Animals were euthanized for whole blood isolation by cardiac puncture and harvesting of various organs of interest (aorta, spleen, and long bone). All animal experiments were performed in compliance with an approved IACUC protocol, according to the University of Pittsburgh Division of Laboratory Animal Resources guidelines.

Lipid and Cytokine/chemokine Analyses. Mouse serum (prepared from whole blood and further diluted with PBS at a 1:1 ratio) were probed for cytokine/chemokine expression levels by

Luminex analysis by service provided by Eve Technologies (Calgary, AB Canada) using MD32 (32-analyte murine discovery panel) panel. For mouse serum analyses, analyte values were normalized to the average of wild-type animals across litters. Lipid panel analysis of mouse serum was performed for low-density lipoprotein (LDL), high-density lipoprotein (HDL), total cholesterol, and triglycerides by the University of Pittsburgh Division of Laboratory Animal Resources (Idexx #6290, Westbrook ME) to confirm lipid elevation in atherosclerotic mice.

Histology and quantification of atherosclerosis parameters. Briefly, cardiac tissue was fixed overnight, maintained in 30% sucrose, and excess cardiac tissue was cut up to the aortic root and cleaned of excess tissue before embedding in OCT for performing 5-10 μm serial sections until the aortic root could be appropriately visualized. These sections were stained for Oil Red-O to visualize lipid accumulation, and Masson's trichrome to visualize the fibrous cap and collagen deposition. These services were performed by the University of Pittsburgh histology core. Total plaque was identified by dark-red area present in Oil Red O staining. Fibrous cap was identified as darkly stained layer present around necrotic core (situated between vascular wall and fibrous cap).

Immunological profiling. Whole blood or various tissues (spleen, thoracic aorta, bone marrow) were crushed and passed through a 70μm cell strainer, treated with 1X red blood cell (RBC) lysis buffer to reduce RBC contamination, and incubated with Brilliant Stain Buffer (BD Biosciences, San Jose, CA) to prevent signal overlap between blue and ultraviolet markers. Samples were stained with either a full panel of immune-cell specific antibodies or buffer only for 30 minutes at 4ºC, spun, and fixed in fixation/permeabilization buffer overnight before staining for various

immunological markers for 30 minutes at room temperature (see [16] for details of immune-panel antibodies and respective dilution for staining). Samples were run on a Fortessa FACS Aria II and the data were analyzed by FlowJo (FlowJo Inc., Ashland, OR) software.

Immunoblot. Total cell lysate (TCL) was collected using a modified RIPA buffer (25 mMTris-HCl, pH 7.5, 150 mM NaCl, 1% (v/v) Nonidet P-40, 5% (v/v) glycerol), 1 mM EDTA, 50 mM NaF, 1 mM sodium pervanadate, along with 6x sample buffer with SDS diluted to 2% in final buffer. For liver extract preparation, mouse liver was cut, digested, and sonicated in lysis buffer for 1 min and spun for 30 min at >8000g. For immunoblotting, antibodies specific for LDLR (BioLegend, ab124904; 1:200), GFP (Living Colors, Takara Biotech, San Jose CA, 632375; 1:2000), Pfn1 (Abcam, ab124904; 1:3000)), and GAPDH (Sigma-Aldrich, G9545; 1:2000) were used.

Statistics. All statistical tests were performed using GraphPad Prism 9 software. For experiments with small sample size and non-normal distribution of data, non-parametric Mann-Whitney u-test was used for statistical comparison of data between the groups. For experiments involving a larger sample size and normal sample distribution, an unpaired t-test was used. Two-way ANOVA was used for multiple group comparison in lipid panel analysis. A p-value less than 0.05 was considered to be statistically significant.

Results and Discussion

To assess the impact of EC-specific Pfn1 depletion on atherosclerosis, we used $Pfn1^{+/-(EC)}$ C57Bl/6 mice for two reasons. Firstly, we recently showed that complete loss of Pfn1 in ECs leads to

mortality within 3 weeks of gene ablation[16] and since it takes several months to develop atherosclerosis in mouse models, Pfn1$^{-/-(EC)}$ mice are not suitable for atherosclerosis development studies. Secondly, use of Pfn1$^{+/-(EC)}$ animals (which are completely viable) allows for a direct evaluation of EC-specific partial depletion of Pfn1 vs previously published global Pfn1 heterozygous knockout mouse model-based findings in atherosclerosis setting[15]. ECs harvested from Pfn1$^{+/-(EC)}$ have ~50% downregulation of Pfn1 expression at the protein level and are morphologically indistinguishable from those harvested from Pfn1$^{+/+}$ mice (**Figs 1A-B**).

Since generating LDLR$^{-/-}$ mice harboring additional cell-type-specific conditional knockout of gene of interest requires extensive breeding and is time consuming, we adopted use of AAV8-mPCSK9 combined with HCD to induce atherosclerosis[20], [21]. PCSK9 directly binds to hepatic LDLR promoting its degradation in the lysosomes, and consequently, induces hyperlipidemia[23]. To initially confirm the efficacy of AAV8-mPCSK9–induced depletion of hepatic LDLR, we probed for expression of LDLR in the liver in both Pfn1$^{+/+}$ and Pfn1$^{+/-(EC)}$ mice 3.5 months after a single intraperitoneal injection of AAV8-mPCSK9 vs AAV8-GFP (as control). Immunoblot analyses of liver extracts showed near complete depletion of LDLR in both Pfn1$^{+/+}$ and Pfn1$^{+/-(EC)}$ mice following administration of AAV8-mPCSK9 (**Fig 1C**). Lipid panel analyses of serum showed significant elevation of both total cholesterol and LDL (but not triglycerides and HDL) in HCD-fed Pfn1$^{+/+}$ and Pfn1$^{+/-(EC)}$ mice which were administered with AAV8-mPCSK9 relative to those receiving AAV8-GFP (**Fig 1D**). However, we did not find any significant difference in the serum level of either total cholesterol or LDL between Pfn1$^{+/+}$ and Pfn1$^{+/-(EC)}$ animals (**Fig 1D**) suggesting that partial loss of EC Pfn1 does not impact the severity of hyperlipidemia. Oil Red-O staining of aortic roots revealed presence of atherosclerotic plaques in both Pfn1$^{+/+}$ and Pfn1$^{+/-(EC)}$

mice (**Fig 1E**). However, when we compared multiple features of atherosclerosis including the areas of total plaque, fibrous cap and necrotic core measured at the aortic root, we did not find any statistically significant difference in any of these parameters between the two Pfn1 genotypes of mice (**Fig 1F**). These data further suggest that partial depletion of Pfn1 in vascular EC alone is not sufficient to confer overall protection against experimentally induced atherosclerosis *in vivo*.

Vascular infiltration of both innate and adaptive immune cells is a key feature of atherosclerosis. In particular, presence of pro-inflammatory M1 macrophages exacerbates the disease progression[24], [25]. The role of cytotoxic CD8+ T cells in atherosclerosis has been debatable in the literature. CD8+ T cell activity induces growth and promote instability (i.e. rupture-prone) of atherosclerotic lesions through lysis of EC and smooth muscle cells[26]. These findings correlate with increased abundance of CD8+ T cells in advanced atherosclerotic lesions[27], and higher circulatory level of CD8+ T cells linked to atherosclerosis development[28] in humans. These results support a pro-atherosclerotic role of CD8+ T cells. However, an inverse correlation between CD8+ T cell and macrophage content in human atherosclerotic aortas, taken together with preclinical evidence for antibody-mediated depletion of CD8+ T cells resulting in reduced plaque stability and increased necrosis and macrophage content in advanced-stage LDLR$^{-/-}$ atherosclerotic animals support a protective role of CD8+ T cells in late-stage atherosclerosis [29]. In general, immunosuppressive action of regulatory T cells (Tregs) inhibits atherosclerosis[30]. Furthermore, B cell-driven antibody response to oxidized LDL (driver of chronic inflammation), and cooperation between B and T cells have been demonstrated to contribute to athero-protective immunity in ApoE$^{-/-}$ mouse model of atherosclerosis [31]. Although our studies showed that partial depletion of EC Pfn1 alone does not ameliorate either hyperlipidemia or the severity of

atherosclerosis, we asked whether haplo-insufficiency of vascular EC Pfn1 has any favorable immunological consequence in the setting of atherosclerosis. Therefore, we performed flow cytometric analysis to obtain immunological profile of spleen, bone marrow, thoracic aorta and whole blood isolated from atherosclerotic $Pfn1^{+/+}$ and $Pfn1^{+/-(EC)}$ mice, and compared the findings from these studies to those obtained in a similar manner for non-atherosclerotic mice (these animals did not receive AAV8-mPCSK9 and were maintained in a normal diet). As summarized in **Fig 2**, we noticed a statistically significant decrease in circulatory cytotoxic CD8+ T cell abundance in atherosclerotic $Pfn1^{+/-(EC)}$ vs $Pfn1^{+/+}$ mice. A similar trend was also observed in the aortic CD8+ T cell population in atherosclerotic mice although the difference did not reach statistical significance likely because of large animal-to-animal variability. Given that this trend was not observed in splenic and bone marrow CD8+ T cell population, it is likely that CD8+ T cell mobilization from lymphoid organs rather than their development was negatively impacted in atherosclerotic $Pfn1^{+/-(EC)}$ mice. It is important to note that non-atherosclerotic mice did not show any effect of partial loss of EC Pfn1 on circulatory and aortic CD8+ T cell abundance (**Fig S1**). When analyzed for relative content of B cells between the two groups of animals, both splenic and aortic B cell content in atherosclerotic $Pfn1^{+/-(EC)}$ mice showed signs of elevation relative to $Pfn1^{+/+}$ animals although the difference did not reach statistical significance because of large animal-to-animal variability (**Fig 2**). Somewhat consistent with these findings, non-atherosclerotic $Pfn1^{+/-(EC)}$ mice also exhibited a sign of elevated circulating B cells relative to $Pfn1^{+/+}$ mice with the p-value close to being significant ($p=0.07$); however, a reverse trend was found when splenic B cell content was compared between the two groups of animals in non-atherosclerosis setting (**Fig S1**). We recently showed that complete loss of vascular EC Pfn1 induces a selective bias of myeloid-derived cells (monocytes/macrophages) toward a pro-inflammatory phenotype *in vivo*[16].

Consistent with these findings, anti-inflammatory Ly6C^{lo} monocytes were present at a lower level in atherosclerotic bone marrow and non-atherosclerotic spleen isolates of Pfn1$^{+/-(EC)}$ relative to Pfn1$^{+/+}$ mice; however, these changes were not preserved in the aortic immune cell compositional analyses (**Fig 2**). In summary, these immunological profiling studies demonstrate that the most noteworthy changes in the immune cell composition of the aorta (the main pathologic tissue of interest) elicited by partial loss of EC Pfn1 in atherosclerosis setting are trends of diminished and elevated CD8+ T cells and B cells, respectively.

To gain further mechanistic insights into how partial loss of EC Pfn1 may alter circulating/aortic composition of select immune cell sub-types in atherosclerosis setting, we performed a broad assessment of circulating cytokine/chemokines in the two groups of animals utilizing a Luminex assay probing for a panel of 32 immunomodulatory factors. As per these analyses, IP-10/CXCL10 and IL7 are the only two immunomodulatory factors that were differentially abundant within statistical significance with the average circulating CXCL10 and IL7 levels being ~40% and ~70% lower, respectively, in Pfn1$^{+/-(EC)}$ relative to Pfn1$^{+/+}$ atherosclerotic animals. (**Figs 3A-B**). Similar Luminex analyses performed with serum of non-atherosclerotic animals did not reveal any significant difference in circulating level of either CXCL10 or IL7 between the two groups, suggesting that the effect of partial loss of EC Pfn1 on these cytokines is specific to atherosclerosis setting (**Figs 3A-B**). CXCL10 is associated with pro-inflammatory immune cell activation, specifically playing a prominent role T cell recruitment in chronic inflammation [32], [33]. A previous study found that genetic ablation of CXCL10 leads to reduced CD8+ T cell accumulation and enhanced Treg activity resulting in a prominent two-fold reduction in atherosclerotic lesion formation in ApoE$^{-/-}$ mice [32]. Reduced circulating CXCL10 level in Pfn1$^{+/-(EC)}$ relative to Pfn1$^{+/+}$

animals specifically in atherosclerosis setting may partly explain diminished circulating and aortic CD8+ T cell abundance as a consequence of partial loss of EC Pfn1. Interestingly, these CXCL10-associated data diverges from our recently published findings of prominent CXCL10 elevation in response to complete loss of EC Pfn1 *in vitro* and *in vivo*[16]. IL7, a cytokine that triggers Th1 and Th17 response [34], has pro-atherogenic function[35]. Overall, these cytokine profiling data demonstrate that partial depletion of EC Pfn1 leads to reduction of select pro-atherogenic cytokines and chemokines in atherosclerosis setting.

In conclusion, this study for the first time investigates the impact of cell-type-specific partial loss of Pfn1 expression on atherosclerosis development. Although changes in EC play a key role in the initiation of atherosclerosis, our studies show that partial loss of Pfn1 expression selectively in ECs has certain beneficial effects (such as dampening of select pro-atherogenic cytokines/chemokines with concomitant reduction in cytotoxic T cell abundance) but is not sufficient to confer atheroprotection *in vivo*. In light of these findings, we conclude that previously reported atheroprotective phenotype of global $Pfn1^{+/-}$ mice [15] is attributed to combined effects of Pfn1 depletion in additional cell types that are relevant for atherosclerosis progression. Therefore, it will be interesting to investigate in the future whether attenuated Pfn1 expression in monocytes/macrophages and/or smooth muscle cells offer additional benefits that could potentially explain atheroprotection conferred by global Pfn1 haplo-insufficiency.

ACKNOWLEDGMENTS

The study was supported by grants from the National Institute of Health (F31HL160118-01-AAG; R01-CA2488373, R01-CA271095 - PR), and the Department of Defense (W81XWH-19-

1-0768 - PR). AAG was also supported by ARCS funding and Cardiovascular Bioengineering T32 training grant from NHLBI (5T32 HL 76124-14).

FIGURE LEGENDS

Figure 1. **Pfn1 haplo-insufficiency in vascular EC is not sufficient to induce atheroprotection**. **A-B)** Immunoblot analyses of Pfn1 (*panel A* – GAPDH: loading control) and phase-contrast images (*panel B*) for CD31+ mouse kidney ECs isolated from $Pfn1^{+/+}$ and $Pfn1^{+/-(EC)}$ mice. **C)** Immunoblot anlsyses of liver extracts prepared from mice of indicated Pfn1 genotypes showing loss of LDLR expression in reponse to AAV8-mPCSK9 administration (samples from AAV8-GFP injected mice serve as control; GAPDH-loading control). **D)** Relative serum levels of total cholesterol, LDL, HDL and triglycerides in AAV8-mPCSK9 vs AAV8-GFP injected mice of indicated Pfn1 genotypes maintained on a high cholesterol diet. The number of animals for various groups for lipid panel analyses were: $Pfn1^{+/+}$/PCSK9 (n=5); $Pfn1^{+/-(EC)}$/PCSK9 (n=5); $Pfn1^{+/+}$/GFP (n=5); $Pfn1^{+/-(EC)}$/GFP (n=3) **E-F)** Representative images of aortic roots prepared from atherosclerotic $Pfn1^{+/+}$ and $Pfn1^{+/-(EC)}$ mice stained with Oil Red-O and Masson's trichrome staining (*panel E*) along with quantifications of various atherosclerosis-related parameters (data normalized to the mean values of $Pfn1^{+/+}$ mice (*panel F*). Data were summarized from 6 $Pfn1^{+/+}$ and 8 $Pfn1^{+/-(EC)}$ atherosclerotic mice pooled from multiple experiments; $^{*}p<0.05$, $^{**}p<0.01$, $^{***}p<0.001$, $^{****}p<0.0001$; ns – not significant.

Figure 2. **Immuneprofiling of athersclerotic $Pfn1^{+/+}$ and $Pfn1^{+/-(EC)}$ mice**. Flow cytometry-based analyses of the relative abundance of various immune cell subtypes (as % of total leukocytes) in the circulation (whole blood) and various organs/tisssues (spleen, aorta and bone marrow) of atherosclerotic $Pfn1^{+/+}$ and $Pfn1^{+/-(EC)}$ ('n' indicates the number of animals in each group pooled from mutiple experiments; 'p' values when significant or close to being significant are indicated).

Figure 3. **Luminex based profiling of circulating cytokines and chemokines of atherosclerotic vs non-atherosclerotic Pfn1$^{+/+}$ and Pfn1$^{+/-(EC)}$ mice**. **A-B)** Heat-plots showing relative abundance of indicated cytokines and chemokines in the serum of atherosclerotic (*panel A*) and non-atherosclerotic (*panel B*) mice of indicated genotypes (data for each analyte normalized to the corresponding mean value calculated of Pfn1$^{+/+}$ mice; immunomodulatory factor(s) that are differentially abundant within statistical significance are indicated by asterisk. **B)** Relative serum abundance of CXCL10 and IL7 between the two groups of animals in atherosclerosis vs non-atherosclerosis settings ('n' indicates the number of animals in each group pooled from mutiple experiments; ns – not significant).

Supplemental data

Figure S1. **Immuneprofiling of non-athersclerotic Pfn1$^{+/+}$ and Pfn1$^{+/-(EC)}$ mice**. Flow cytometry-based analyses of the relative abundance of various immune cell subtypes (as % of total leukocytes) in the circulation (whole blood) and various organs/tisssues (spleen, aorta and bone marrow) of non-atherosclerotic Pfn1$^{+/+}$ and Pfn1$^{+/-(EC)}$ ('n' indicates the number of animals in each group pooled from mutiple experiments; 'p' values when significant or close to being significant are indicated).

REFERENCES

[1] World Health Organization, "Cardiovascular diseases." Accessed: Aug. 04, 2023. [Online]. Available: https://www.who.int/health-topics/cardiovascular-diseases

[2] D. Shepard, A. VanderZanden, A. Moran, M. Naghavi, C. Murray, and G. Roth, "Ischemic Heart Disease Worldwide, 1990 to 2013," *Circ. Cardiovasc. Qual. Outcomes*, vol. 8, no. 4, pp. 455–456, Jul. 2015, doi: 10.1161/CIRCOUTCOMES.115.002007.

[3] A. J. Lusis, "Atherosclerosis," *Nature*, vol. 407, no. 6801, pp. 233–241, Sep. 2000, doi: 10.1038/35025203.

[4] R. Ross, "The pathogenesis of atherosclerosis: a perspective for the 1990s," *Nature*, vol. 362, no. 6423, pp. 801–809, Apr. 1993, doi: 10.1038/362801a0.

[5] A. Sharma *et al.*, "Direct Endothelial Nitric Oxide Synthase Activation Provides Atheroprotection in Diabetes-Accelerated Atherosclerosis," *Diabetes*, vol. 64, no. 11, pp. 3937–50, Jun. 2015, doi: 10.2337/db15-0472.

[6] S. Kawashima and M. Yokoyama, "Dysfunction of endothelial nitric oxide synthase and atherosclerosis," *Arterioscler. Thromb. Vasc. Biol.*, vol. 24, no. 6, pp. 998–1005, Mar. 2004, doi: 10.1161/01.ATV.0000125114.88079.96.

[7] S. Cejkova, I. Kralova-Lesna, and R. Poledne, "Monocyte adhesion to the endothelium is an initial stage of atherosclerosis development," *Cor Vasa*, vol. 58, no. 4, pp. e419–e425, Aug. 2016, doi: https://doi.org/10.1016/j.crvasa.2015.08.002.

[8] B. O. Oluwole, W. Du, I. Mills, and B. E. Sumpio, "Gene regulation by mechanical forces," *Endothel. J. Endothel. Cell Res.*, vol. 5, no. 2, pp. 85–93, 1997, doi: 10.3109/10623329709079866.

[9] T. N. Dear, N. T. Meier, M. Hunn, and T. Boehm, "Gene structure, chromosomal localization, and expression pattern of Capn12, a new member of the calpain large subunit gene family," *Genomics*, vol. 68, no. 2, pp. 152–160, Sep. 2000, doi: 10.1006/geno.2000.6289.

[10] A. Schaefer *et al.*, "Actin-binding proteins differentially regulate endothelial cell stiffness, ICAM-1 function and neutrophil transmigration," *J. Cell Sci.*, vol. 127, no. 20, pp. 4470–4482, Oct. 2014, doi: 10.1242/jcs.154708.

[11] I. Tabas, X. Zha, N. Beatini, J. N. Myers, and F. R. Maxfield, "The actin cytoskeleton is important for the stimulation of cholesterol esterification by atherogenic lipoproteins in macrophages.," *J. Biol. Chem.*, vol. 269, no. 36, pp. 22547–22556, Sep. 1994, doi: 10.1016/S0021-9258(17)31681-2.

[12] F. Y. McWhorter, T. Wang, P. Nguyen, T. Chung, and W. F. Liu, "Modulation of macrophage phenotype by cell shape," *Proc. Natl. Acad. Sci. U. S. A.*, vol. 110, no. 43, pp. 17253–17258, Oct. 2013, doi: 10.1073/pnas.1308887110.

[13] E. Caglayan *et al.*, "Profilin-1 is expressed in human atherosclerotic plaques and induces atherogenic effects on vascular smooth muscle cells," *PloS One*, vol. 5, no. 10, p. e13608, Oct. 2010, doi: 10.1371/journal.pone.0013608.

[14] R. Wang, G. Liao, Y. Wang, and D. D. Tang, "Distinctive roles of Abi1 in regulating actin-associated proteins during human smooth muscle cell migration," *Sci. Rep.*, vol. 10, no. 1, p. 10667, Jun. 2020, doi: 10.1038/s41598-020-67781-1.

[15] G. R. Romeo, K. S. Moulton, and A. Kazlauskas, "Attenuated Expression of Profilin-1 Confers Protection From Atherosclerosis in the LDL Receptor–Null Mouse," *Circ. Res.*, vol. 101, pp. 357–367, Jun. 2007, doi: 10.1161/CIRCRESAHA.107.151399.

[16] A. Allen-Gondringer *et al.*, "Vascular endothelial cell-specific disruption of the profilin1 gene leads to severe multiorgan pathology and inflammation causing mortality," *PNAS Nexus*, vol. 2, no. 10, p. pgad305, Sep. 2023, doi: 10.1093/pnasnexus/pgad305.

[17] D. Gau *et al.*, "Disruption of profilin1 function suppresses developmental and pathological retinal neovascularization," *J. Biol. Chem.*, vol. 295, no. 28, pp. 9618–9629, Jul. 2020, doi: 10.1074/jbc.RA120.012613.

[18] A. Allen *et al.*, "Actin-binding protein profilin1 promotes aggressiveness of clear-cell renal cell carcinoma cells," *J. Biol. Chem.*, vol. 295, no. 46, pp. 15636–15649, Nov. 2020, doi: 10.1074/jbc.RA120.013963.

[19] D. Gau *et al.*, "Pharmacological intervention of MKL/SRF signaling by CCG-1423 impedes endothelial cell migration and angiogenesis," *Angiogenesis*, vol. 20, no. 4, pp. 663–672, Nov. 2017, doi: 10.1007/s10456-017-9560-y.

[20] S. Kumar, D.-W. Kang, A. Rezvan, and H. Jo, "Accelerated atherosclerosis development in C57Bl6 mice by overexpressing AAV-mediated PCSK9 and partial carotid ligation," *Lab. Invest.*, vol. 97, no. 8, Art. no. 8, Aug. 2017, doi: 10.1038/labinvest.2017.47.

[21] N. Zelcer and M. Westerterp, "Adeno-Associated Viruses as a Method to Induce Atherosclerosis in Mice and Hamsters," *Circ. Res.*, vol. 114, no. 11, pp. 1672–1674, May 2014, doi: 10.1161/CIRCRESAHA.114.304067.

[22] A. O'Doherty, M. Rosenblat, M. Aviram, and T. O'Brien, "114. AAV-Mediated Delivery of Paraoxonase 1 (PON1) to the ApoE-/- Mouse as Gene Therapy for Atherosclerosis," *Mol. Ther.*, vol. 15, p. S45, May 2007, doi: 10.1016/S1525-0016(16)44320-0.

[23] E. Yurtseven, D. Ural, K. Baysal, and L. Tokgözoğlu, "An Update on the Role of PCSK9 in Atherosclerosis," *J. Atheroscler. Thromb.*, vol. 27, no. 9, pp. 909–918, Sep. 2020, doi: 10.5551/jat.55400.

[24] M. J. Davies, "Stability and instability: two faces of coronary atherosclerosis. The Paul Dudley White Lecture 1995," *Circulation*, vol. 94, no. 8, pp. 2013–2020, Oct. 1996, doi: 10.1161/01.cir.94.8.2013.

[25] E. K. Koltsova *et al.*, "Dynamic T cell–APC interactions sustain chronic inflammation in atherosclerosis," *J. Clin. Invest.*, vol. 122, no. 9, pp. 3114–3126, Sep. 2012, doi: 10.1172/JCI61758.

[26] T. Kyaw *et al.*, "Cytotoxic and proinflammatory CD8+ T lymphocytes promote development of vulnerable atherosclerotic plaques in apoE-deficient mice," *Circulation*, vol. 127, no. 9, pp. 1028–1039, Mar. 2013, doi: 10.1161/CIRCULATIONAHA.112.001347.

[27] J. Gewaltig, M. Kummer, C. Koella, G. Cathomas, and B. C. Biedermann, "Requirements for CD8 T-cell migration into the human arterial wall," *Hum. Pathol.*, vol. 39, no. 12, pp. 1756–1762, Dec. 2008, doi: 10.1016/j.humpath.2008.04.018.

[28] J. Podolec *et al.*, "Higher levels of circulating naïve CD8+CD45RA+ cells are associated with lower extent of coronary atherosclerosis and vascular dysfunction," *Int. J. Cardiol.*, vol. 259, pp. 26–30, May 2018, doi: 10.1016/j.ijcard.2018.01.079.

[29] J. van Duijn *et al.*, "CD8+ T-cells contribute to lesion stabilization in advanced atherosclerosis by limiting macrophage content and CD4+ T-cell responses," *Cardiovasc. Res.*, vol. 115, no. 4, pp. 729–738, Apr. 2019, doi: 10.1093/cvr/cvy261.

[30] A. C. Foks, A. H. Lichtman, and J. Kuiper, “Treating atherosclerosis with regulatory T cells,” *Arterioscler. Thromb. Vasc. Biol.*, vol. 35, no. 2, pp. 280–287, Feb. 2015, doi: 10.1161/ATVBAHA.114.303568.

[31] G. Caligiuri, A. Nicoletti, B. Poirier, and G. K. Hansson, “Protective immunity against atherosclerosis carried by B cells of hypercholesterolemic mice,” *J. Clin. Invest.*, vol. 109, no. 6, pp. 745–753, Mar. 2002, doi: 10.1172/JCI7272.

[32] E. A. Heller *et al.*, “Chemokine CXCL10 Promotes Atherogenesis by Modulating the Local Balance of Effector and Regulatory T Cells,” *Circulation*, vol. 113, no. 19, pp. 2301–2312, May 2006, doi: 10.1161/CIRCULATIONAHA.105.605121.

[33] R. Li *et al.*, “Interleukin-7 induces recruitment of monocytes/macrophages to endothelium,” *Eur. Heart J.*, vol. 33, no. 24, pp. 3114–3123, Dec. 2012, doi: 10.1093/eurheartj/ehr245.

[34] A. Bikker, C. E. Hack, F. P. J. G. Lafeber, and J. A. G. van Roon, “Interleukin-7: a key mediator in T cell-driven autoimmunity, inflammation, and tissue destruction,” *Curr. Pharm. Des.*, vol. 18, no. 16, pp. 2347–2356, 2012, doi: 10.2174/138161212800165979.

[35] P. M. Mihailovic *et al.*, “IL-7R blockade reduces post-myocardial infarction-induced atherosclerotic plaque inflammation in ApoE-/- mice,” *Biochem. Biophys. Rep.*, vol. 19, p. 100647, Sep. 2019, doi: 10.1016/j.bbrep.2019.100647.

Allen-Gondringer et al. Fig 1

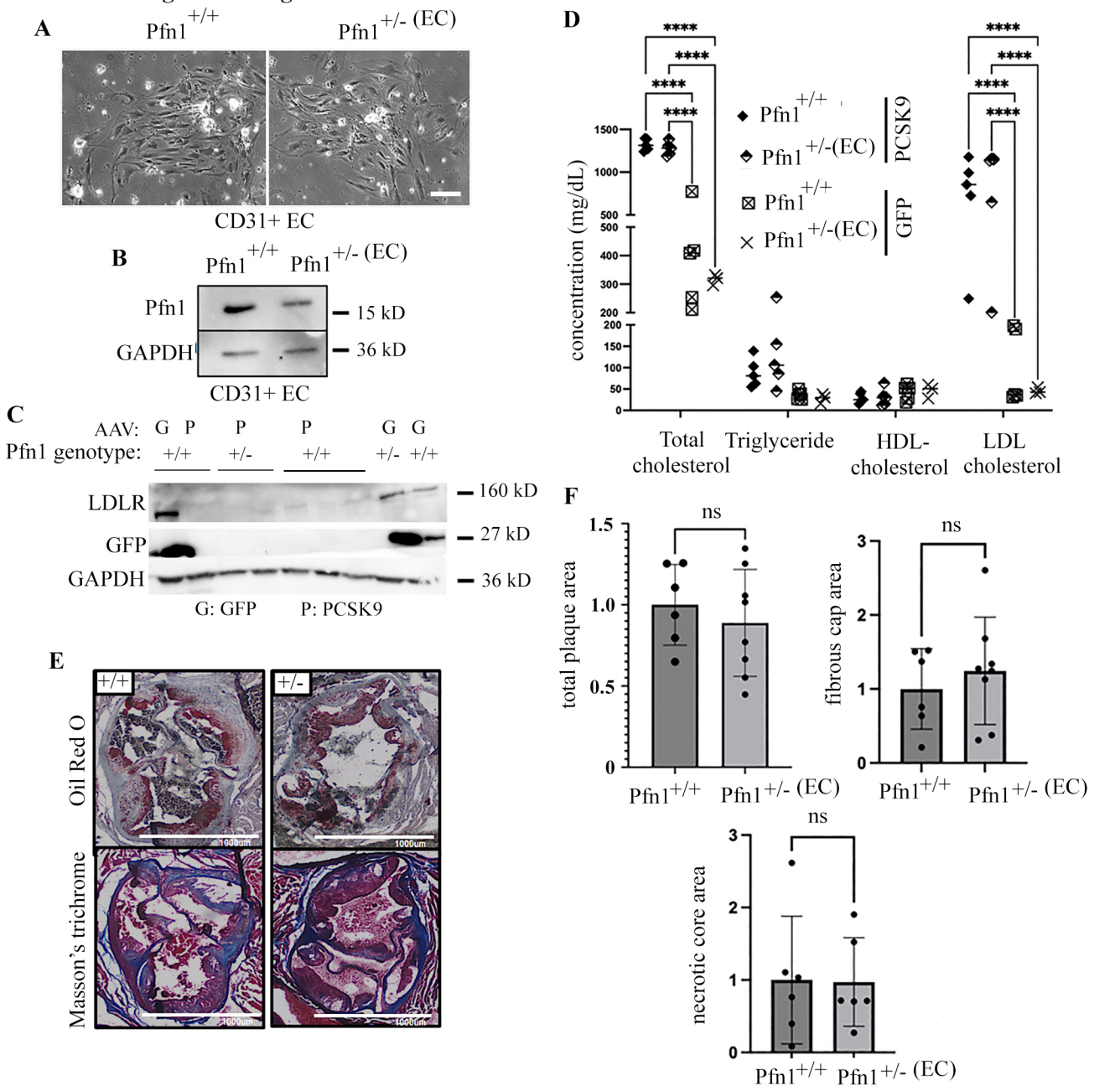

Allen-Gondringer et al. Fig 2

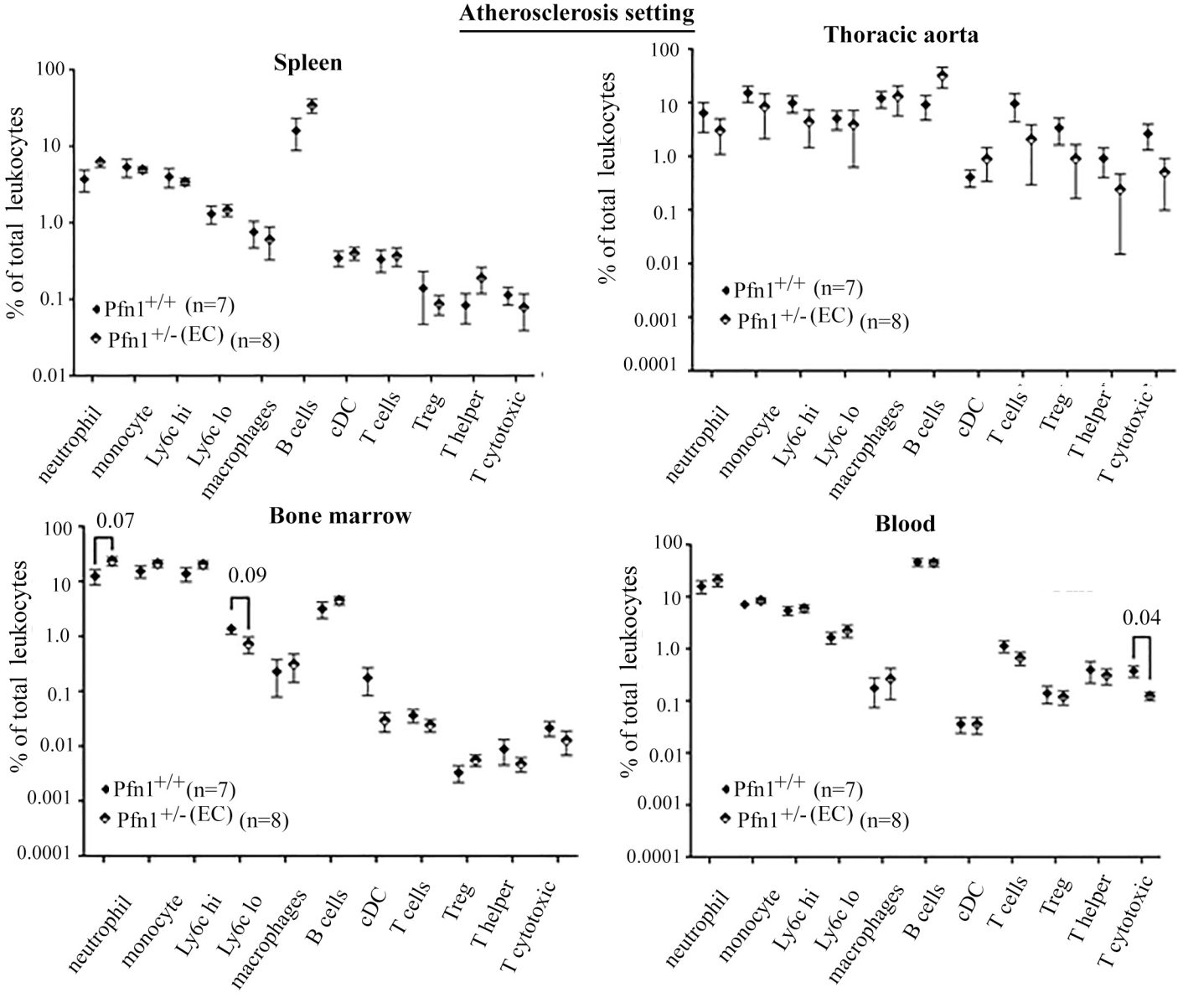
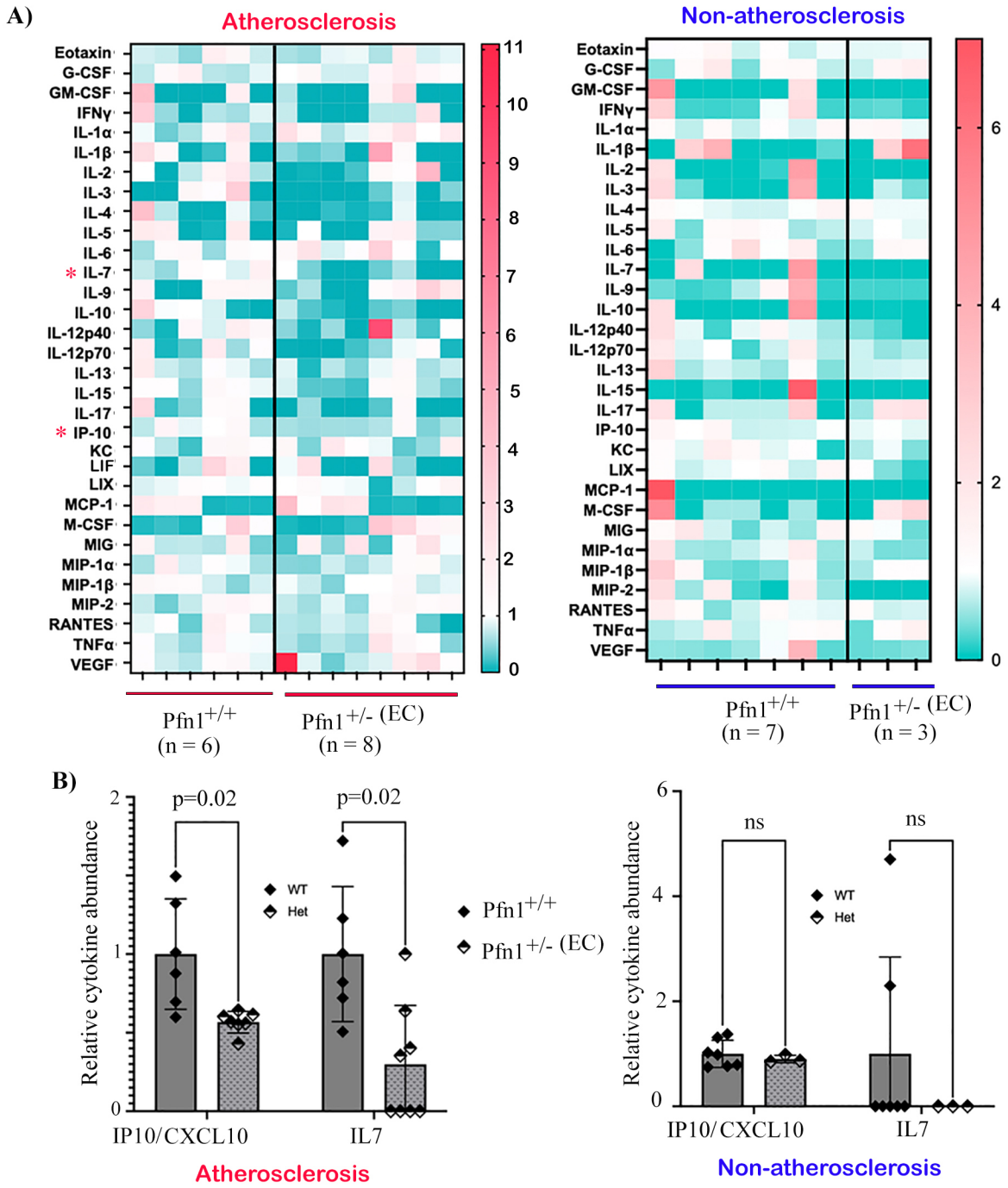
Allen-Gondringer et al. Fig 3